

Electronic Supplementary Information

Boosting of overall water splitting activity by regulating electron distribution over active site of Ce doped NiCo-LDH and atomic level understanding of the catalyst by DFT study

**Hariharan N Dhandapani,^{†‡} D. Mahendiran,^{†@} Arun Karmakar,^{†‡} P. Devi,^{†@}
Sreenivasan Nagappan,^{†‡} Ragunath Madhu,^{†‡} Krishnendu Bera,^{†‡} Palanichamy
Murugan,^{†@*} B. Ramesh Babu^{†‡*} and Subrata Kundu^{†‡*}**

[†]*Academy of Scientific and Innovative Research (AcSIR), Ghaziabad-201002, India.*

[‡]*Electrochemical Process Engineering (EPE) Division, CSIR-Central Electrochemical Research Institute (CECRI), Karaikudi-630003, Tamil Nadu, India.*

[@]*Electrochemical Power Sources (ECPS) Division, CSIR-Central Electrochemical Research Institute (CECRI), Karaikudi-630003, Tamil Nadu, India.*

*To whom correspondence should be addressed, *E-mail:* murugan@cecri.res.in; brbabu@cecri.res.in; skundu@cecri.res.in; kundu.subrata@gmail.com; Phone/Fax: (+ 91) 4565-241487.

This file contains 24 pages which contains the details of reagents, electrochemical results, electrochemical characterizations, characterizations like XRD, post SEM and EDS spectra results are provided.

Figures	Subject of the Figure	Page number
S1	XRD spectra of NiCo-LDH, 8.5%, 17% and 25.5% Ce@NiCo-LDH in Nickel foam	4
S2	EDS spectrum of (a) NiCo-LDH/NF (b) 25.5% Ce@NiCo-LDH/NF from FESEM showing the presence of expected elements.	5
S3	Combined XPS spectra of Ce@NiCo-LDH/NF	6
S4	Bar diagram of OER overpotential of NiCo-LDH/NF, 8.5% ,17% and 25.5% of Ce@NiCo-LDH/NF	7
S5	The area of Reduction peak of A) NiCo-LDH/NF (B-D) 8.5%, 17% and 25.5% Ce doped NiCo-LDH/NF	10
S6	The electrochemically effective surface area of A) NiCo-LDH/NF (B-D) 8.5%, 17% and 25.5% Ce@NiCo-LDH/NF in OER.	11
S7	ECSA normalized LSV polarisation curve plot of NiCo-LDH/NF, 8.5%, 17% and 25.5% Ce@NiCo-LDH/NF.	12
S8	OER polarisation curve of 25.5% Ce doped NiCo-LDH/NF before and after AD	13
Table S1	Comparison table for OER activity of Ce@NiCo-LDH/NF with similar type of catalyst.	14
S9	Bar diagram of HER overpotential of NiCo-LDH/NF, 8.5% ,17% and 25.5% of Ce@NiCo-LDH/NF	15
Table S2	Comparison table for HER activity of Ce@NiCo-LDH/NF with similar type of catalyst.	16
Table S3	Comparison table for total water splitting of Ce@NiCo-LDH/NF with similar type of catalyst	17
S10	Ball and stick models for optimized structure of (A) Ni _{2/3} Co _{1/3} (OH) ₂ (Co atoms replacing nearby Ni atoms).	18
S11	(A-C) SEM image of Post OER characterization of Ce@NiCo-LDH/NF (D-E) FESEM image of Post OER characterization of Ce@NiCo-LDH/NF.	19
S12	(A-B) Post OER HR-TEM images of Ce@NiCo-LDH/NF (C) the corresponding lattice fringes of the post OER sample (D) SAED pattern for the post-OER sample (E) Post OER HAADF image of Ce@NiCo-LDH/NF obtained for the mapping analysis (F-G) the characteristic colour mapping results for O, Ce, Ni and Co.	20
S14	(A)Non deconvoluted XPS spectra of Ni 2p orbitals (B) Ce 3d orbitals and (C) O 1s orbitals of NiCo-LDH/NF and Ce@ NiCo-LDH/NF before and after OER.	22
	References	

Reagents and Instruments:

Nickel nitrate Hexahydrate ($\text{Ni}(\text{NO}_3)_2 \cdot 6\text{H}_2\text{O}$), Cobalt nitrate Hexahydrate ($\text{Co}(\text{NO}_3)_2 \cdot 6\text{H}_2\text{O}$), Urea, Cerium nitrate Hexahydrate ($\text{Ce}(\text{NO}_3)_3 \cdot 6\text{H}_2\text{O}$), Ammonium fluoride (NH_4F) were purchased from Sigma-Aldrich and used as received. 1N HCl, Ethanol and Acetone were purchased from Merck and used as received. Ni foam was purchased from Sigma-Aldrich and used after surface cleaning. The electrochemical analyser AURT-M204 was used for all electrochemical characterizations. Hg/HgO reference electrode (1M KOH) from CH instruments and platinum as counter electrode from Alfa-Aesar were used throughout the electrochemical studies. The entire experiments were conducted using deionised water. Characterization of the catalyst was done by HR-TEM, (TecnaiTM G² TF20), operating at an accelerating voltage of 200 kV and elemental color mapping by Talos F-200-S with HAADF. Energy Dispersive X-ray Spectroscopy (EDS) analysis was performed by SUPRA 55VP Carl Zeiss with a separate EDS detector. Scanning Electron Microscopy (SEM) analysis was carried with a Hitachi, Japan (Model S-3000H) having magnification varying from 30X to 300 KX with the accelerating voltage ~ 0.3 to 30 kV. XRD analysis was carried out with a scanning rate of 5°min^{-1} in the 2θ range 10 - 90° using a Rigaku X-ray powder diffractometer (XRD) with Cu K_α radiation ($\lambda = 0.154 \text{ nm}$).

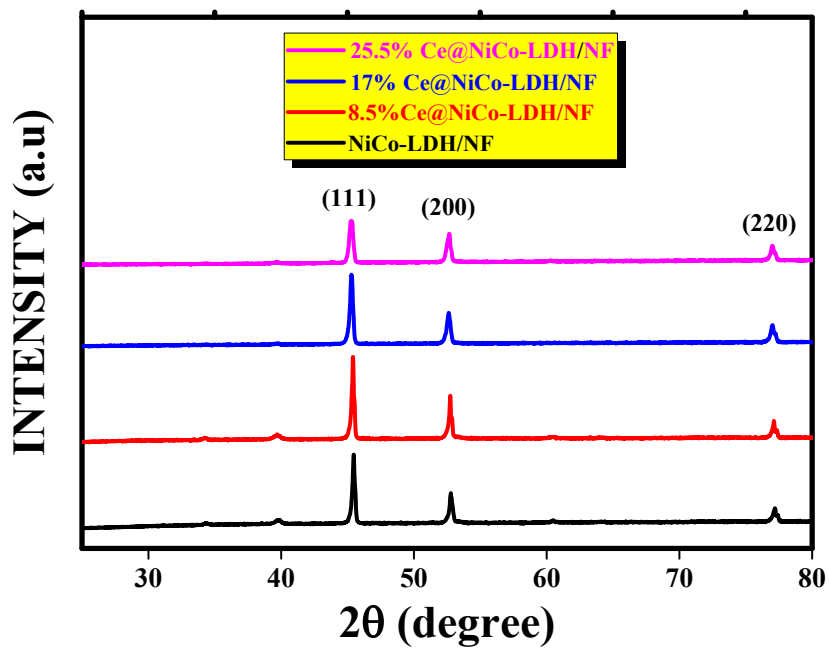


Figure S1: XRD spectra of NiCo-LDH, 8.5%, 17% and 25.5% Ce@NiCo-LDH in Nickel foam.

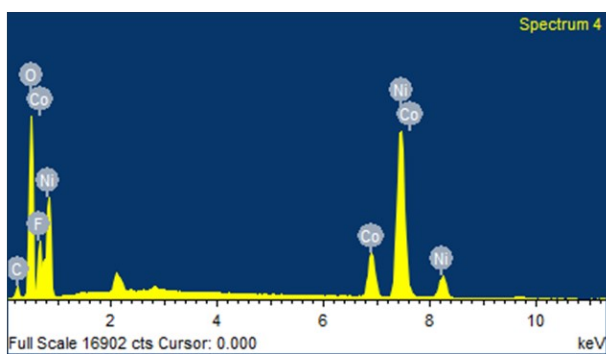
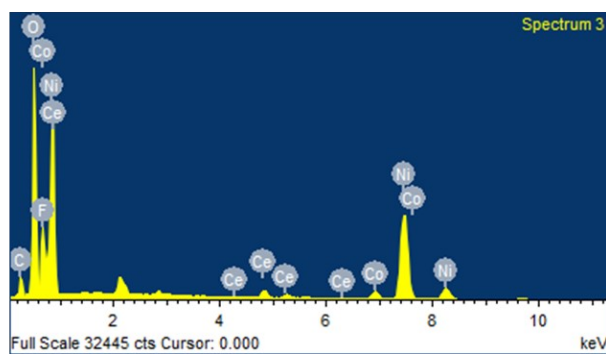
A**B**

Figure S2: EDS spectrum of (a) NiCo-LDH/NF (b) 25.5% Ce@NiCo-LDH/NF from FESEM showing the presence of expected elements.

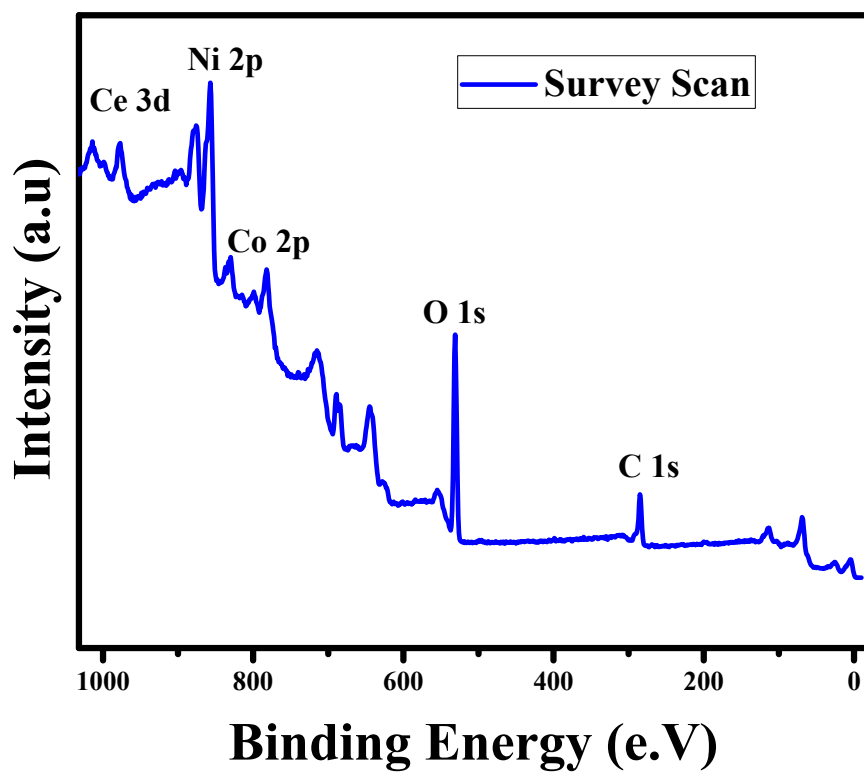


Figure S3: Combined XPS spectra of Ce@NiCo-LDH/NF.

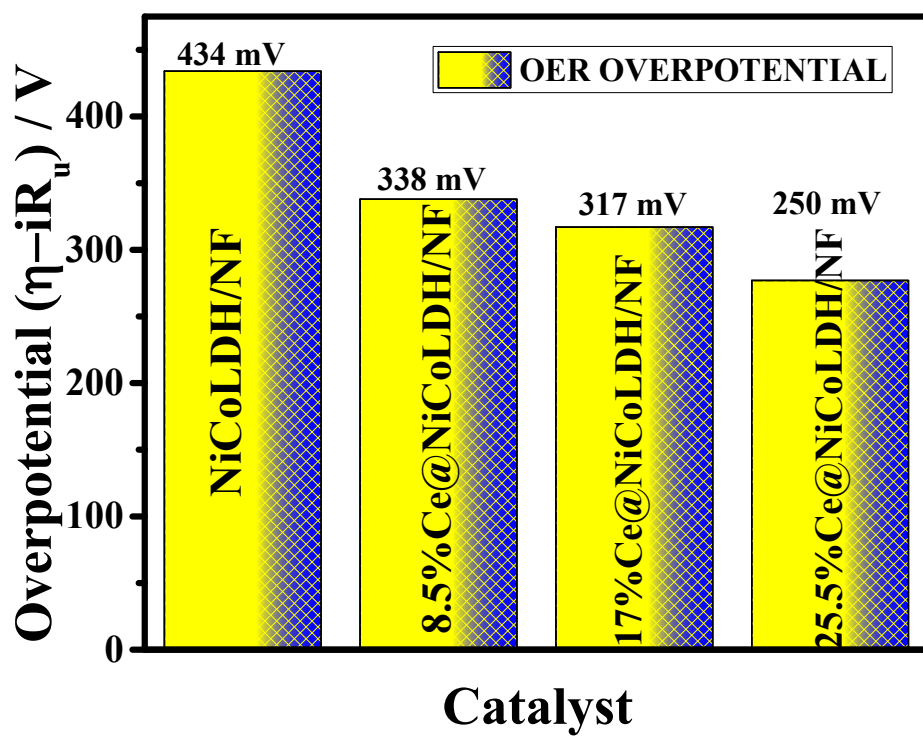


Figure S4: Bar diagram of OER overpotential of NiCo-LDH/NF, 8.5%, 17% and 25.5% of Ce@NiCo-LDH/NF.

Determination of Surface concentration of various alloys from the redox features of CV^{1,2}:

- Calculated area associated with the oxidation of Ni³⁺ to Ni²⁺ of **NiCo-LDH** = 0.00287 VA

Hence, the associated charge is = 0.0287 VA / 0.005 Vs⁻¹

$$= 5.56 \text{ As}$$

$$= \mathbf{5.56C}$$

Now, the number of electron transferred is = 5.586 C / 1.602 × 10⁻¹⁹

$$= \mathbf{3.45 \times 10^{19}}$$

Since, the reduction of Ni³⁺ to Ni²⁺ is a single electron transfer reaction, the number of electrons calculated above is exactly the same as the number of surface-active sites.

Hence, the number of Ni participate in OER is = **3.45 × 10¹⁹**

Hence, Determination of Turnover Frequency (TOF) from OER Current Density TOF in our study was calculated assuming that the surface-active Co atoms that had undergone the redox reaction just before onset of OER only participated in OER electrocatalysis. The corresponding expression is,

$$\text{TOF} = j \times N_A / F \times n \times \Gamma$$

Where, j = current density N_A = Avogadro number F = Faraday constant n = Number of electrons Γ = Surface concentration.

$$\text{TOF} = [(3.91 \times 10^{-3}) (6.023 \times 10^{23})] / [(96485) (4) (3.45 \times 10^{19})]$$

$$= \mathbf{0.000176 \text{ sec}^{-1}}$$

- Calculated area associated with the oxidation of Ni³⁺ to Ni²⁺ of **25.5%Ce@NiCo-LDH** = 0.0373VA

Hence, the associated charge is = 0.0373VA / 0.005 Vs⁻¹

$$= 7.46 \text{ As}$$

$$= \mathbf{7.46 C}$$

Now, the number of electron transferred is = $7.46 \text{ C} / 1.602 \times 10^{-19}$

$$= 4.636 \times 10^{19}$$

Since, the reduction of Ni^{3+} to Ni^{2+} is a single electron transfer reaction, the number of electron calculated above is exactly the same as the number of surface-active sites.

Hence, the number of Ni participate in OER is = 4.636×10^{19}

Hence, we have,

$$\text{TOF} = [(51 \times 10^{-3}) (6.023 \times 10^{23})] / [(96485) (4) (4.636 \times 10^{19})]$$

$$= 0.00171 \text{ sec}^{-1}$$

Similarly, TOF values were calculated for 8.5% Ce@NiCo-LDH and 17% Ce@NiCo-LDH and they were $0.000549 \text{ sec}^{-1}$ and $0.000923 \text{ sec}^{-1}$.

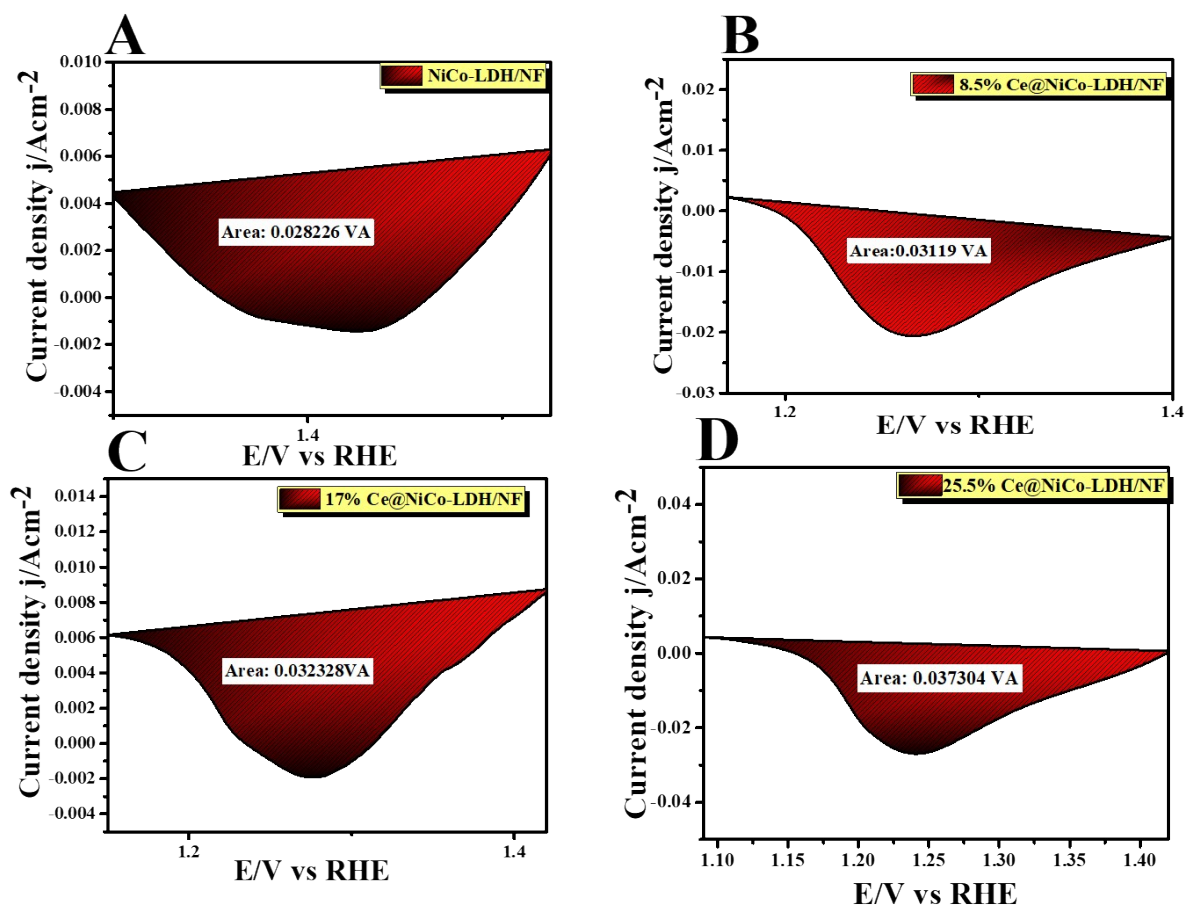


Figure S5: The area of Reduction peak of A) NiCo-LDH/NF (B-D) 8.5%, 17% and 25.5% Ce doped NiCo-LDH/NF.

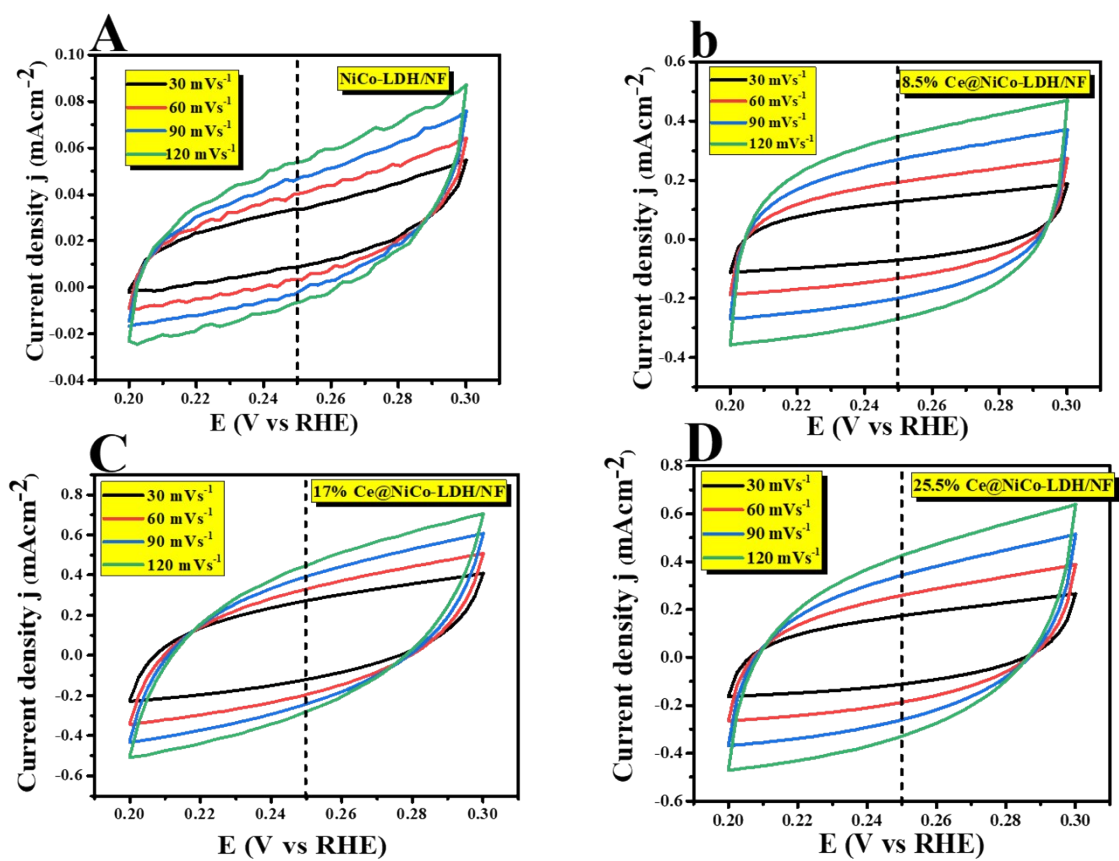


Figure S6: The electrochemically effective surface area of A) NiCoLDH/NF (B-D) 8.5%,17% and 25.5% Ce@NiCo-LDH/NF in OER.

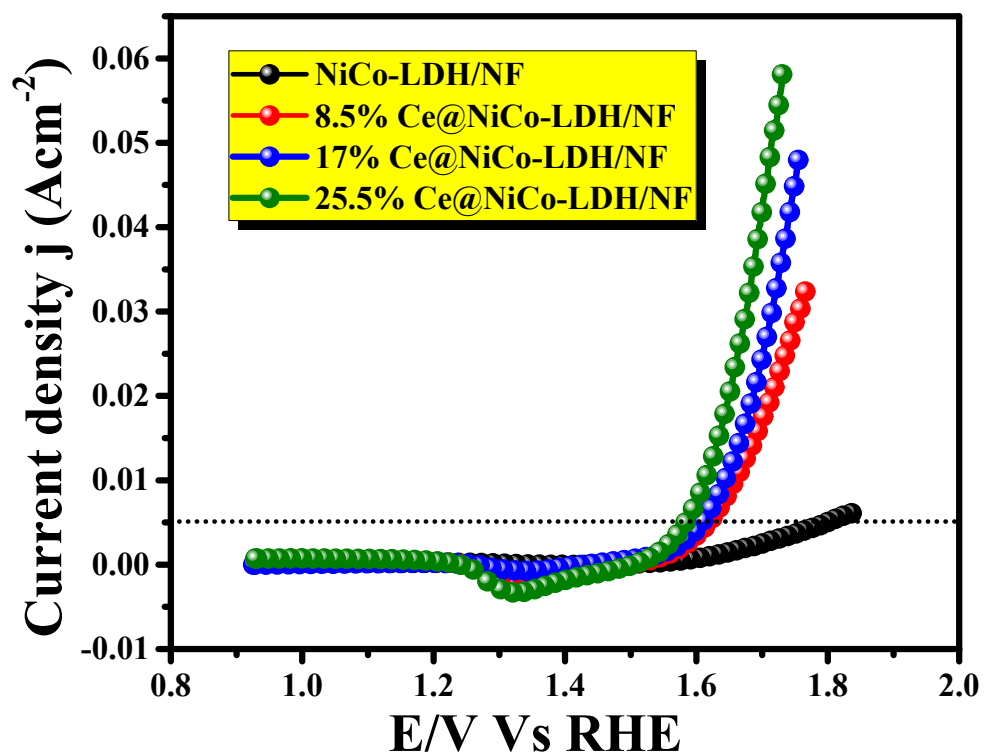


Figure S7: ECSA normalized LSV polarisation curve plot of NiCo-LDH/NF, 8.5%, 17% and 25.5% Ce@NiCo-LDH/NF.

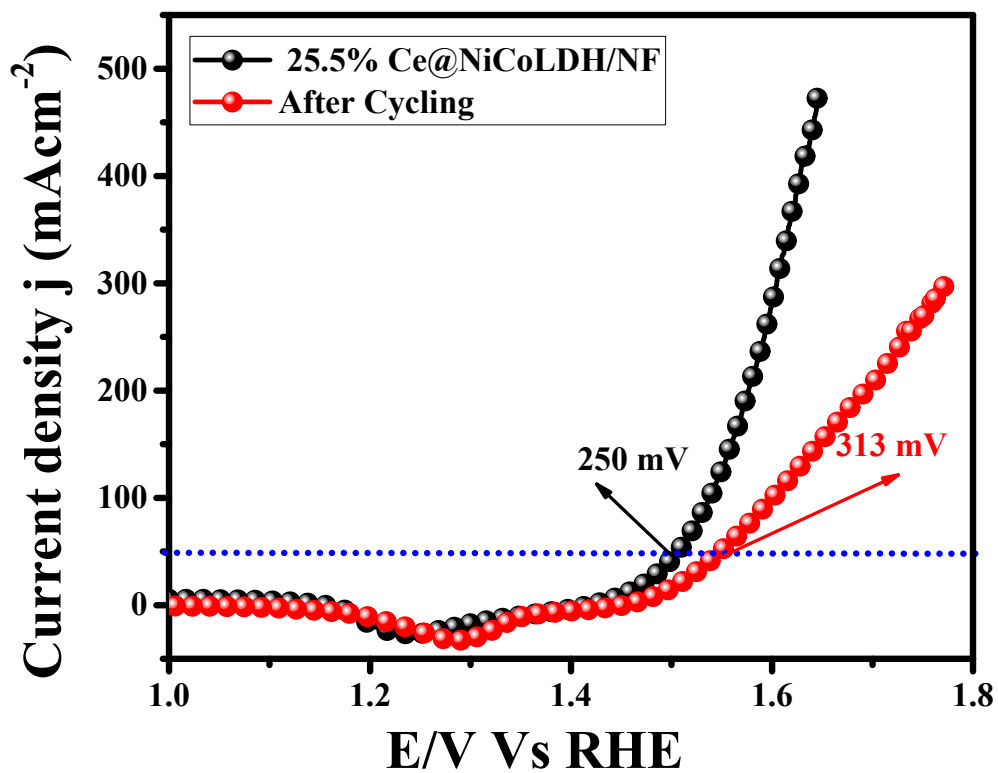


Figure S8: OER polarisation curve of 25.5% Ce doped NiCo-LDH/NF before and after AD.

Table S1: Comparison table for OER activity of Ce@NiCo-LDH/NF with similar type of catalyst.

3

SI.No	Catalyst	Overpotential (mV)	Tafel slope (mV/dec)	Current density (mA/cm ²)	Reference
1	ZnCo-LDH/Ni foil	520	83	10	1
2	Fe ³⁺ rich CoFe-LDH	310	-	10	2
3	CoFe Borate-LDH	418	131	10	3
4	NiCo ₂ S ₄ @Co ₁ Ni ₄ -LDH	337	112	100	4
5	CoFe-LDH on graphene	330	43	10	5
6	CdS@NiCo-LDH/NF	198	39	100	7
7	Ni ₄ Co ₂ Fe ₃ - LDH	320	65	10	7
8	CoFe LDH/rGO	396	43	10	5
9	Exfoliated NiCo- LDH	334	41	10	8
10	Ce@NiCo-LDH/NF	250	98	50	This work

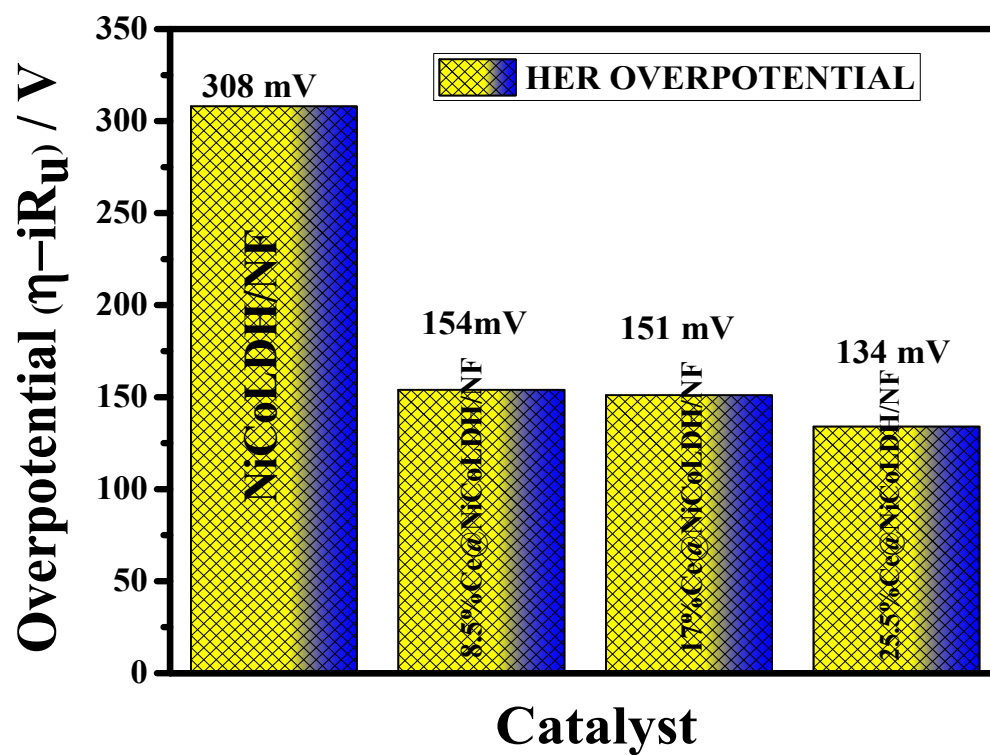


Figure S9: Bar diagram of HER overpotential of NiCo-LDH/NF, 8.5%, 17% and 25.5% of Ce@NiCo-LDH/NF.

Table S2: Comparison table for HER activity of Ce@NiCo-LDH/NF with similar type of catalyst.

Sl.No	Catalyst	Overpotential (mV)	Tafel slope (mV/dec)	Current density (mA/cm ²)	Reference
1	CoFe-OH/Ni foam	110	72	10	9
2	NiFeCo LDH	108	73	10	9
3	Ni ₃ S ₂ /Cu-NiCo LDH/NF	156	129	10	10
4	CoMoV LDH/NF	150	182	10	11
5	CoFe LDH @g-C ₃ N ₄	210	79	10	12
6	NiCo-OH	350	150	10	13
7	Ce@NiCo-LDH/NF	134	98.6	50	This work

Table S3: Comparison table for total water splitting of Ce@NiCo-LDH/NF with similar type of catalyst.

SI.No	Catalyst	Potential (mV)	Electrolyte	Current density (mA/cm ²)	Reference
1	Ni _{0.75} Fe _{0.125} V _{0.125} -LDHs/NF	1.591	1.0M KOH	10	14
2	Co@Ir/NC-x	1.7	1.0M KOH	10	15
3	Ni ₃ S ₂ /Cu-NiCo LDH/NF	1.75	1.0M KOH	100	5
4	Ni ₃ Se ₄ @NiFe LDH	1.54	1.0M KOH	10	16
5	Ce@NiCo-LDH/NF	1.68	1.0M KOH	10	This work

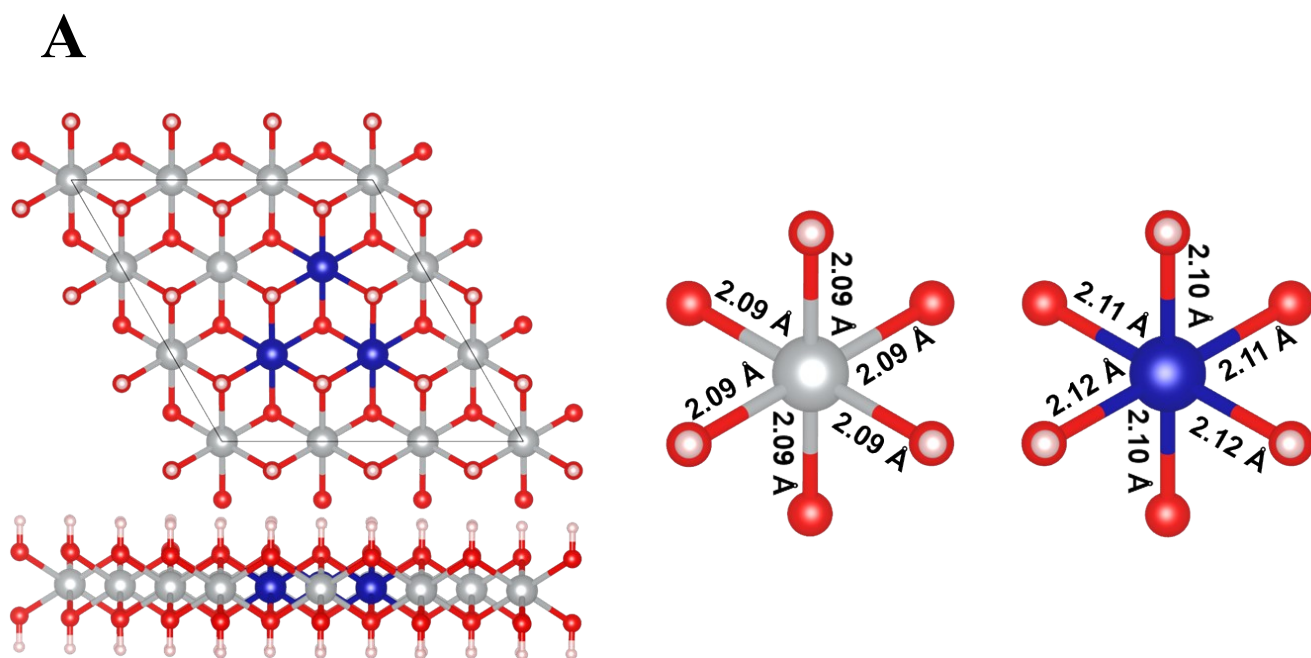


Figure S10: Ball and stick models for optimized structure of (A) $\text{Ni}_{2/3}\text{Co}_{1/3}(\text{OH})_2$ (Co atoms replacing nearby Ni atoms). The blue, grey, and red color balls represent Co, Ni, and O, respectively. A comparison of the octahedral bond distances of NiO_6 and CoO_6 .

Computational Methodology:

In this work, first principles density functional theory (DFT) approach was carried out by employing the plane-wave based formalism, as implemented in the Vienna Ab initio Simulation Packages (VASP)¹⁹. The electron–electron interactions were corrected by generalized gradient approximations (GGA) in the scheme of Perdew–Burke–Ernzerhof,²⁰ and ion–electron interactions, were described by projector-augmented wave (PAW) approach. The kinetic energy cut-off of 400 eV was used for plane-wave expansion and the total free energies in all the cases were converged below 10^{-5} eV. Iterative relaxation processes were repeated until a Hellman-Feynman force of atoms along any axis was converged below to $0.01 \text{ eV}/\text{\AA}$. To avoid interaction between real system and its periodic images, vacuum thickness placed in the z-direction was kept to be $> 15\text{\AA}$. Gamma centred K-grid of $3 \times 3 \times 1$ is used for optimizing $3 \times 3 \times 1$ surface slab. The entire DFT calculations were performed by the spin-polarized calculations in which initial moment of all transition metal atoms, was set

to be aligned parallel to one another. VESTA was used to render all of the atomic models as well as the spin density.²¹

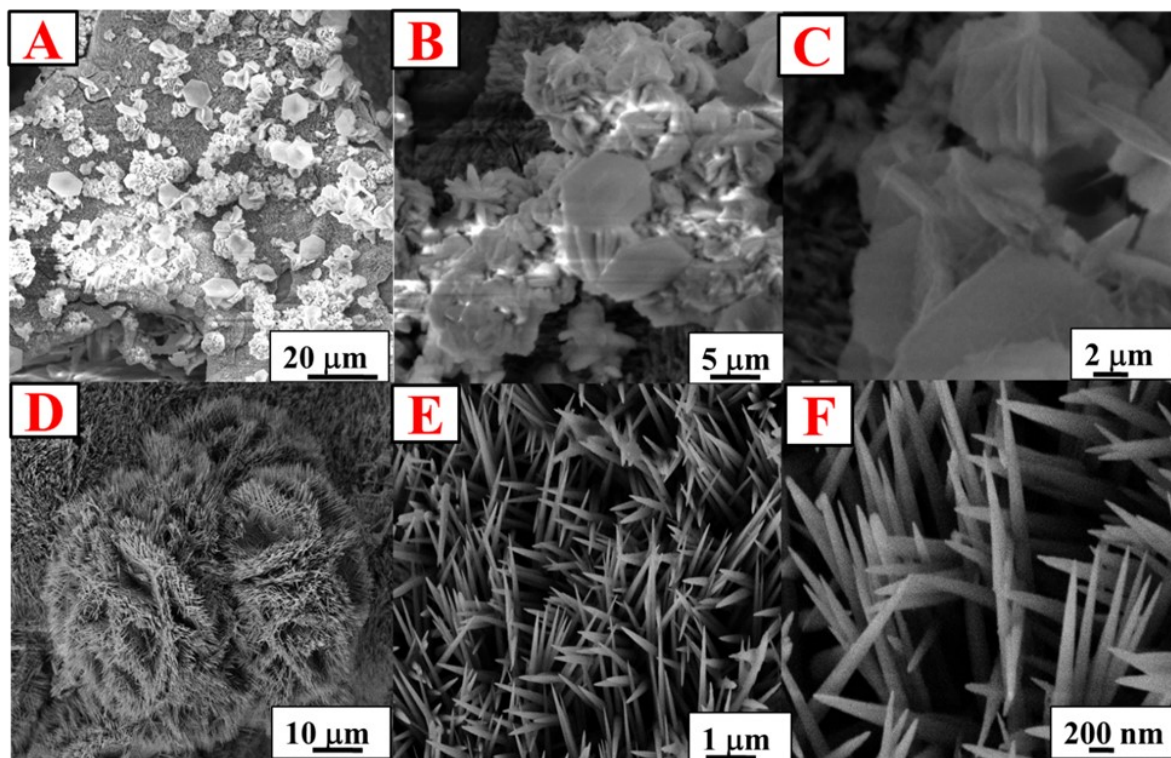


Figure S11: (A-C) SEM image of Post OER characterization of Ce@NiCo-LDH/NF (D-E) FESEM image of Post OER characterization of Ce@NiCo-LDH/NF.

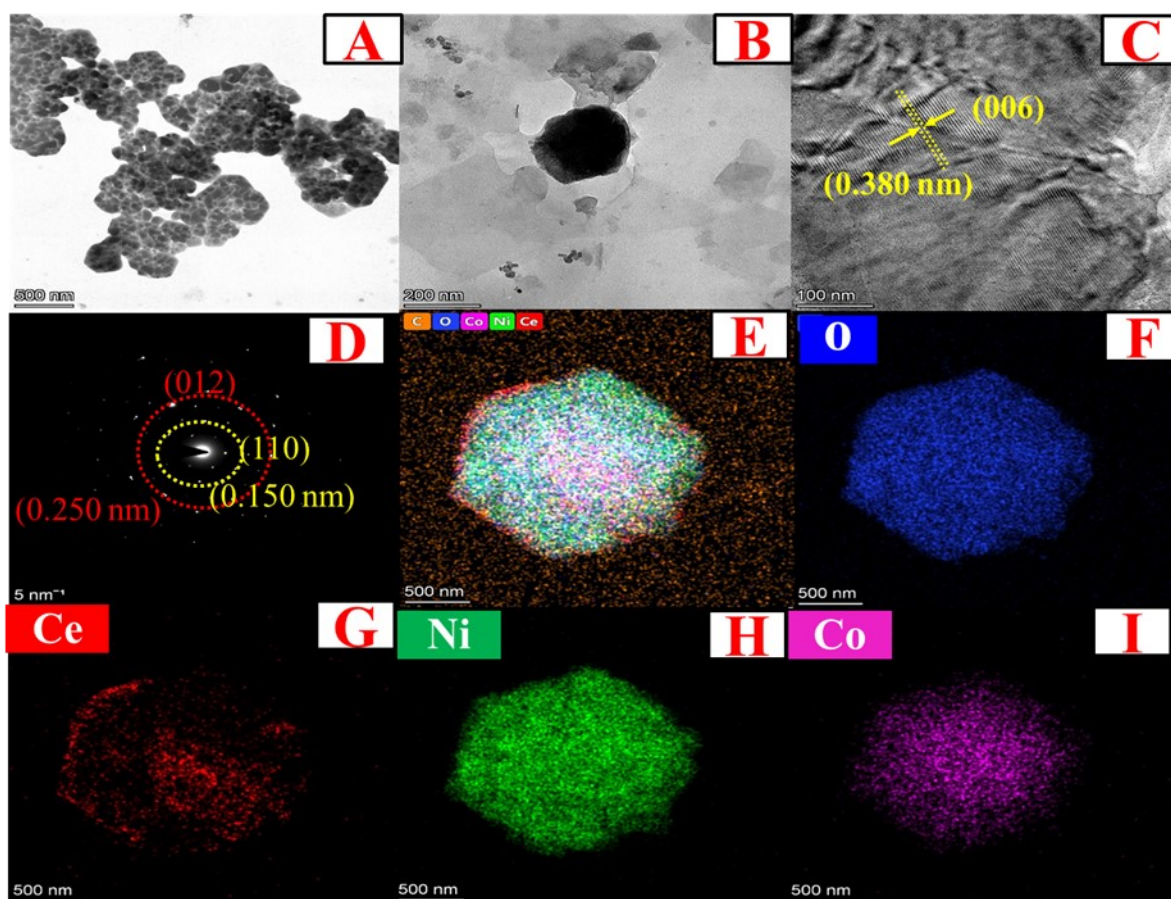


Figure S12: (A-B) Post OER HR-TEM images of Ce@NiCo-LDH/NF (C) the corresponding lattice fringes of the post OER sample (D) SAED pattern for the post-OER sample (E) Post OER HAADF image of Ce@NiCo-LDH/NF obtained for the mapping analysis (F-G) the characteristic colour mapping results for O, Ce, Ni and Co.

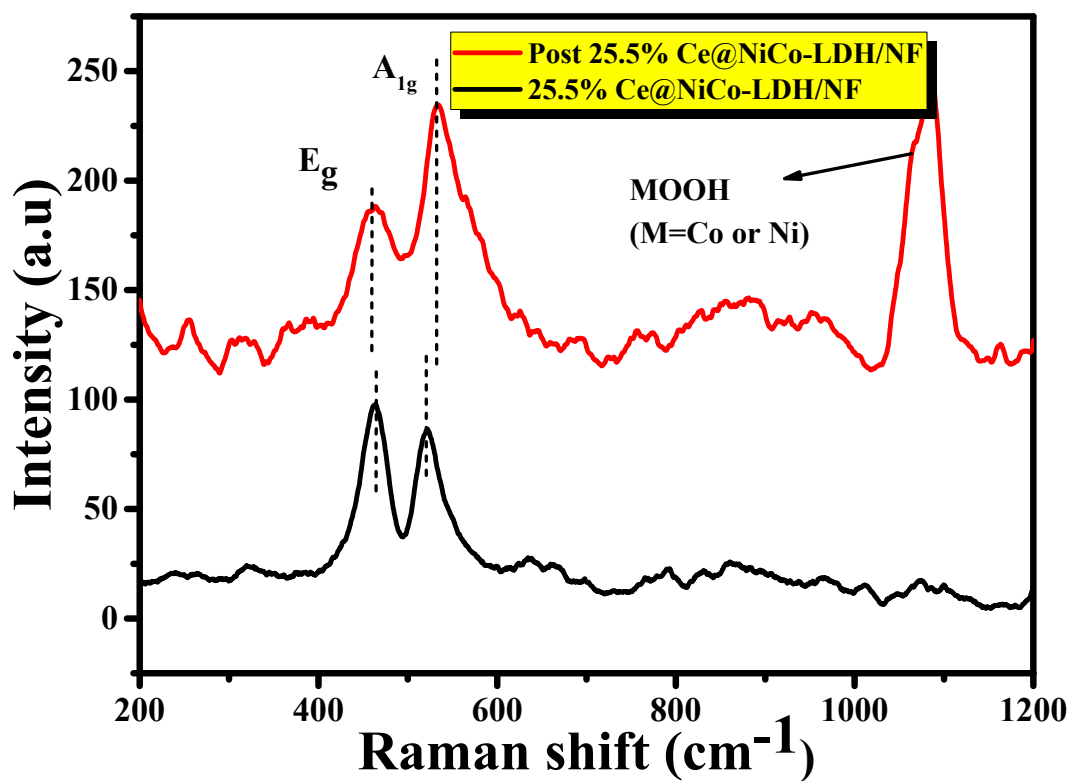


Figure S13: Raman spectrum of 25.5% Ce doped NiCo-LDH/NF before and after the OER study.

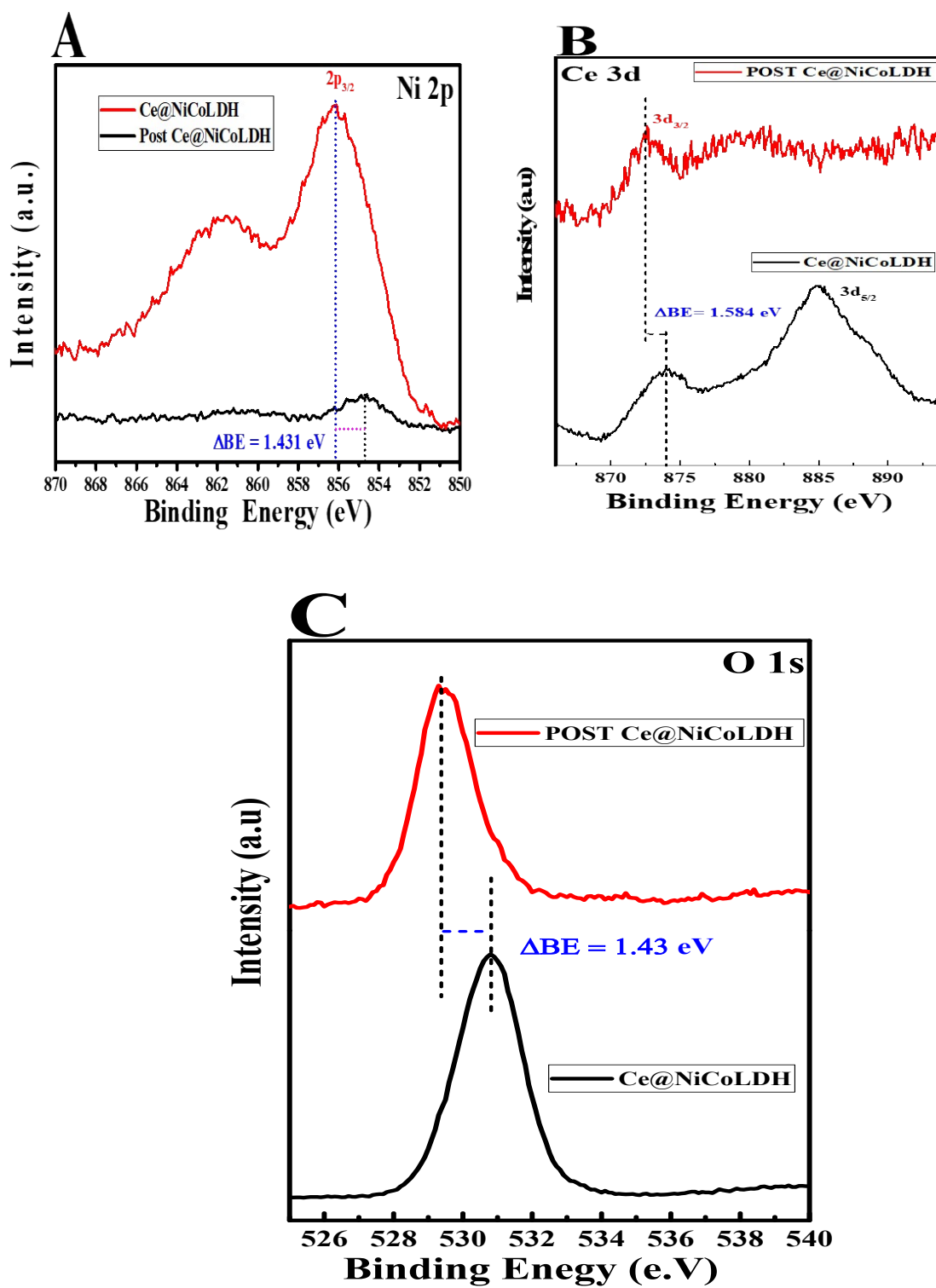


Figure S14: (A) Non deconvoluted XPS spectra of Ni 2p orbitals; (B) Ce 3d orbitals and (C) O 1s orbitals of NiCo-LDH and Ce@ NiCo-LDH/NF before and after OER.

REFERENCES:

- 1 S. Anantharaj and S. Kundu, *ACS Energy Letters*, 2019, **4**, 1260–1264.
- 2 K. Karthick, S. Anantharaj, P. E. Karthik, B. Subramanian and S. Kundu, *Inorganic Chemistry*, 2017, **56**, 6734–6745.
- 3 A. Guzmán-Vargas, J. Vazquez-Samperio, M. A. Oliver-Tolentino, N. Nava, N. Castillo, M. J. Macías-Hernández and E. Reguera, *Journal of Materials Science*, 2018, **53**, 4515–4526.
- 4 Y. Li, L. Zhang, X. Xiang, D. Yan and F. Li, *Journal of Materials Chemistry A*, 2014, **2**, 13250–13258.
- 5 S. Weiß, M. Ertl, S. D. Varhade, A. v. Radha, W. Schuhmann, J. Breu and C. Andronescu, *Electrochimica Acta*, , DOI:10.1016/j.electacta.2020.136256.
- 6 C. You, Y. Ji, Z. Liu, X. Xiong and X. Sun, *ACS Sustainable Chemistry and Engineering*, 2018, **6**, 1527–1531.
- 7 F. Yuan, J. Wei, G. Qin and Y. Ni, *Journal of Alloys and Compounds*, , DOI:10.1016/j.jallcom.2020.154658.
- 8 X. Han, C. Yu, J. Yang, C. Zhao, H. Huang, Z. Liu, P. M. Ajayan and J. Qiu, *Advanced Materials Interfaces*, , DOI:10.1002/admi.201500782.
- 9 A. Pirkarami, S. Rasouli and E. Ghasemi, *Applied Catalysis B: Environmental*, 2019, **241**, 28–40.
- 10 H. Liang, F. Meng, M. Cabán-Acevedo, L. Li, A. Forticaux, L. Xiu, Z. Wang and S. Jin, *Nano Letters*, 2015, **15**, 1421–1427.
- 11 P. Babar, A. Lokhande, H. H. Shin, B. Pawar, M. G. Gang, S. Pawar and J. H. Kim, *Small*, , DOI:10.1002/sml.201702568.
- 12 L. Jia, G. Du, D. Han, Y. Hao, W. Zhao, Y. Fan, Q. Su, S. Ding and B. Xu, *Journal of Materials Chemistry A*, 2021, **9**, 27639–27650.

- 13 J. Bao, Z. Wang, J. Xie, L. Xu, F. Lei, M. Guan, Y. Zhao, Y. Huang and H. Li, *Chemical Communications*, 2019, **55**, 3521–3524.
- 14 T. Bhowmik, M. K. Kundu and S. Barman, *ACS Applied Energy Materials*, 2018, **1**, 1200–1209.
- 15 S. Baranton and C. Coutanceau, *Applied Catalysis B: Environmental*, 2013, **136–137**, 1–8.
- 16 K. N. Dinh, P. Zheng, Z. Dai, Y. Zhang, R. Dangol, Y. Zheng, B. Li, Y. Zong and Q. Yan, *Small*, , DOI:10.1002/sml.201703257.
- 17 D. Li, Z. Zong, Z. Tang, Z. Liu, S. Chen, Y. Tian and X. Wang, *ACS Sustainable Chemistry and Engineering*, 2018, **6**, 5105–5114.
- 18 T. Zhang, L. Hang, Y. Sun, D. Men, X. Li, L. Wen, X. Lyu and Y. Li, *Nanoscale Horizons*, 2019, **4**, 1132–1138.
- 19 G. Kresse and J. Furthmü, *Efficient iterative schemes for ab initio total-energy calculations using a plane-wave basis set*, 1996.
- 20 J. P. Perdew, J. A. Chevary, S. H. Vosko, K. A. Jackson, M. R. Pederson, D. J. Singh and C. Fiolhais, *Atoms, molecules, solids, and surfaces: Applications of the generalized gradient approximation for exchange and correlation*, vol. 46.
- 21 K. Momma and F. Izumi, *Journal of Applied Crystallography*, 2011, **44**, 1272–1276.